Case Studies in Construction Materials 13 (2020) e00394

Contents lists available at ScienceDirect

Case Studies in Construction Materials

journal homepage: www.elsevier.com/locate/cscm

Case study

Assessment of activity moduli and acidic resistance of slag-based geopolymer concrete incorporating pozzolan

Solomon Oyebisi[a,*], Anthony Ede[a], Festus Olutoge[b], David Olukanni[a]

[a] Department of Civil Engineering, Covenant University, PMB 1023, Km 10, Idiroko Road, Ota, Nigeria
[b] Department of Civil and Environmental Engineering, University of the West Indies, St Augustine, Trinidad and Tobago

ARTICLE INFO

Article history:
Received 25 March 2020
Received in revised form 6 May 2020
Accepted 5 June 2020

Keywords:
Pozzolan
Ground granulated blast furnace slag
Geopolymer concrete
Chemical composition
Alkaline solutions
Flexural strength
Regression models

ABSTRACT

The environmental impact of Portland cement production and utilization in the construction sector has led to the global call for the use of eco-friendly construction materials for the production of cleaner and sustainable products. Therefore, this study explored agro-industrial wastes, slag and corncob ash, for the production of geopolymer concrete (GPC). Corncob was dehydroxylated at 600 °C for 3 h and partially used as a replacement for slag at 0%, 20 %, 40 %, 60 %, 80 %, and 100 %. A 12 M, 14 M, and 16 M of both sodium silicate (SS) and sodium hydroxide (SH) were used as activators. The chemical moduli of each and mixed binder were quantified and evaluated based on the major reactive oxides, hence leading to the evaluation of reactivity indexes (RIs). Moreover, the RIs and mix design properties (MDPs) of concrete were used for the prediction of flexural strength while the chemical resistance of each concrete sample was investigated. Compared with the experimental results, the predictive flexural strengths based on the RIs and the MDPs yielded a high precision with R^2 ranging from 88–92 % at 7–90 days, respectively. Moreover, the GPC, unlike Portland cement concrete (PCC), resisted the more acidic attack. Therefore, the use of GGBFS–CCA blended concrete would be more advantageous in a highly acidic environment than PCC. Ultimately, the models proposed by this study can be useful in the concrete mix design procedure for the flexural strength development of GPC incorporating agro-industrial provided the oxide compositions of each and mixed material were obtained.

1. Introduction

In the construction sector, the utilized rate of concrete is high, owing to the rapid industrialization and urbanization [1]. Amongst the concrete constituents, Portland cement (PC) plays a pivotal role in determining the quality of concrete. However, the production of PC, apart from its negative impact on the environment, requires a massive industrial process [2]. A ton of PC production, which emits 1 ton of carbon dioxide (CO_2) into the atmosphere, requires 4000 MJ energy, 1.5 tons of raw materials, and 140 kW h of electricity [3]. Moreover, a 7–9 % of CO_2 is emitted yearly into the atmosphere following the massive requirements of energy in PC production, hence contributing to the serious global warming [4]; this poses huge threats to human and ecosystem survival and development. Besides, from the building activities alone, Mahmoudkelaye et al. [5] estimated 30–40% generation of greenhouse gas (GHG) emissions, globally. Moreover, the yearly utilization of PCC in the construction industry is estimated to be 20 billion tons globally [6]. Furthermore, the need for the construction of

* Corresponding author.
E-mail address: solomon.oyebisi@covenantuniversity.edu.ng (S. Oyebisi).

https://doi.org/10.1016/j.cscm.2020.e00394
2214-5095/

infrastructures in fast-growing cities could emit 226 gigatonnes of CO_2 by 2050 in the developing nations [6]. Following this trend, the carbon budget of 800 gigatonnes of total CO_2 emissions targeted by the Paris Climate Agreement after 2017 would be challenging to achieve.

In the construction sector, such as concrete mix design [7], pavement engineering [8], and geotechnical engineering [9], sustainable development and production have been a major priority. In the construction sector, there is a global call for the reduction of CO2 emissions associated with PC production. The utilization of supplementary cementitious materials (SCMs) such as fly ash [1,10], coal ash [11], silica fume [1,12], metakaolin (MK) [10] ground granulated blast furnace slag (GGBFS) [10,12], rice husk ash (RHA) [13,14], corncob ash (CCA) [15–17], cashew nutshell ash (CNSA) [18], bagasse ash (BA) [11], palm oil fuel ash (POFA) [19], and cassava peel ash (CPA) [20] in the production of sustainable construction materials, have been yielding favourable results in the recent studies. The partial or full incorporation of SCMs for the green concrete production, apart from limiting the environmental impact of PCC, has been reported to improve the workability [21,22]; mechanical [23,24]; durability [23,25]; and economical [26,27] properties. Moreover, the use of SCMs does not only reduce the initial CO_2 emissions of PC production but also reduce the volume of PCC needed in the construction industry and extend the building's service life [4]. It is interesting to note that in 2016 and 2017 alone, the global production of corn was 969.69 and 1071.51 million metric tons, respectively [28]. Notwithstanding, most of the corncobs produced are discarded as waste, hence culminating in environmental pollution; this justified the recycling of CCA for GPC production. Besides, CCA possesses high silica and alumina contents, hence contributing to its strong pozzolanic response [15,21].

Different techniques have been used to correlate both mechanical and mix properties of concrete. Hammoudi et al. [29] applied artificial neural networks (ANNs) and response surface methodology (RSM) to evaluate the compressive strength (fc) of concrete. It was discovered that ANNs yielded better accuracy than RSM. Moreover, Al-Shamiri et al. [30] adopted an extreme learning approach (ELA) to predict the fc of high-strength concrete. It was revealed that ELA yielded acceptable precision to correlate the fc of high-strength concrete and the mix design proportions. Sobhani et al. [31] used the regression models to predict the fc of no-slump concrete and compared with ANNs and adaptive network-based fussy inference systems (ANFIS). It was inferred from the findings of the study that ANNs and ANFIS yielded better accuracy than regression models. However, the regression models offered a predictive equation for fc based on mix design proportion, while ANNs and ANFIS could not offer such an equation. Oyebisi et al. [18] and Xie and Visintin [14] applied the reactivity, hydraulic, and lime moduli to predict the relationship between the fc of concrete blended with SCMs and the mix design proportions such as water-to-binder ratio and binder-to-aggregate volume ratio of 0.618 and 0.30–1.5, and 0.12 and 0.045 to 0.359, respectively; the predictions yielded good accuracy with 99.66 % and 83.70 % coefficients of determination, respectively. Furthermore, the activity index of any SCM is influenced by its oxide composition, mineralogical composition, fineness, and specific surface area [32,33]. Besides, type, mineralogical, and chemical compositions of aggregates influence the performance and reactivity of concrete [34,35]. However, a single oxide cannot be used to quantify the reactivity of SCM. Hence reactivity, hydraulic, and lime moduli are majorly applied to quantify the hydraulic or self-cementitious properties, while both silica and alumina moduli are commonly used to determine pozzolanic properties [36,37].

Several standards have established the procedures of assessing the chemical indexes and hydraulic efficiency index of GGBFS [38,39] and the pozzolanic activity of pulverized fly ash or natural pozzolan [40,41]. ASTM C 989 [39] classifies GGBFS into three grades (80, 100, and 120) based on the mortar strength of slag activity index (SAI). The SAI for grade 80, 100, and 120, using 50 % cement replacement by the mass of the binding materials at both 7 days and 28 days must be 70 % and 80 %, 70 % and 90 %, and 90 % and 110 % strength minimum of the reference-cement mortar, respectively. Moreover, based on the caustic soda test in assessing the hydraulic activity of slag, ASTM C 1073−18 [42] recommends the compressive strengths of 7 MPa and 8 MPa, and 12 MPa and 15 MPa after 6 h and 8 h hardening, respectively. On the other hand, BS 3892−1 [40] specifies a SAI greater than 0.80 as a positive pozzolanic activity for fly ash or natural pozzolan for 30 % cement replacement after 7 days and 28 days. In contrast, ASTM C 618 [43] recommends a SAI greater than 0.75 for 20 % cement replacement after 7 days and 28 days. Despite the satisfactory and positive results of using chemical indexes and established procedure in assessing both hydraulic and pozzolanic properties of SCMs, there was no literature related to the activity indexes and durability properties of GPC incorporating GGBFS and CCA.

Many of the previous studies considered fc as the most remarkable factor to determine the quality of the concrete mixture [30,31]. Still, another factor, such as flexural strength (fr) has not been considered. Therefore, this paper provides new insight into the oxide compositions of each binding material by using the x-ray fluorescence analyzer (XRF); this guides in assessing the hydraulic and pozzolanic activities of GPC blended with agro-industrial wastes using the RI's concept. It also provides an evaluation of the reactivity of each and blended binding material using the existing RIs, which are commonly used in self-cementitious and pozzolanic reactions; it develops a model to predict the fr of GPC blended with SCMs following the RI and mix design proportions, and investigates the performance of concrete produced under acidic attacks. In achieving these objectives, agro-industrial wastes such as GGBFS and CCA were harnessed, recycled, activated with alkaline solutions, and cured under ambient conditions. The experimental data for flexural strengths were obtained through laboratory work, while the predictive flexural strength was developed via the fit regression model in Minitab 17 to offer a predictive equation [31]. The hydraulic and pozzolanic activity tests of the binding materials were also examined using slag activity index and CST, and SAI and FT, respectively. Slag activity index and CST were adopted because they have been standardized and offered satisfactory results [37–39,42]. In the same vein, both SAI and FT have been standardized, reported, and significantly correlated [37], hence justifying their adoption in this present study. The recycling of both GGBFS and CCA would lessen the environmental, economic, and societal threats posed by the PC production; improve the concrete properties, and reduce the

construction cost and solid wastes, hence driving sustainability. The models developed from this study would enhance the findings of future studies on GPC incorporating SCMs by providing means of predicting fr based on RIs and MDPs.

2. Materials and methods

2.1. Materials

The locally sourced materials, GGBFS and CCA, as shown in Fig. 1, were used as SCMs for the production of GPC, while Portland limestone cement (PLC), as shown in Fig. 1, was used as a binder for the production of PCC and compared with GPC. Slag was ground to obtain GGBFS. Corncob was dehydroxylated at 600 °C for 3 h to obtain CCA. The SCMs were then sieved with BS 90 μm to obtain a similar fineness with PLC.

The specific gravity (SG) of the binding materials was determined following the requirements stated in BS EN 196−3 [44] using a specific gravity bottle and kerosene. The results indicated 2.90 g/cm^3, 2.44 g/cm^3, and 3.15 g/cm^3 for GGBFS, CCA, and PLC, respectively. Owing to these results, GGBFS met the SG limit of 2.90 g/cm^3 to 3.15 g/cm^3 specified by BS EN 15167−1 [38], while that of CCA confirmed the similar results obtained by Oyebisi et al. [21].

The fineness of binding materials was determined using the dry sieving method, and BS sieve 90 μm as stipulated by BS EN 196−6 [45]. The results showed 7.6 %, 8.0 %, and 7.5 % for GGBFS, CCA, and PLC, respectively, hence satisfying the 12 % maximum fineness specification prescribed by BS EN 196−6 [45]. Therefore, the materials are suitable for use as binder and SCMs in concrete production. Furthermore, Laser diffraction, Model Beckman Coulter LS-100, was used to analyze the particle size distribution of the binding materials, as shown in Fig. 2, over the range size of 0.5 μm–900 μm. The results indicated a mean particle size of 20.68 μm, 23.45 μm, and 18.79 μm for GGBFS, CCA, and PLC, respectively. Besides, the specific surface area was carried out on the binding materials following the procedure stated by BS EN 196−6 [45] using the Blaine method at a standard porosity of 0.500. The results indicated 420 m^2/kg, 625 m^2/kg, and 375 m^2/kg for GGBFS, CCA, and PLC, respectively.

The alkaline solutions, SH pellets with 99 % purity, and SS gel were locally sourced and used as activators. SS gel comprises Na_2O, SiO_2, and H_2O of 9.4 %, 30.1 %, and 60.5 % respectively, with SiO_2/Na_2O weight ratio of 3.20 and S.G. of 1.40 g/cm^3 at 20 °C. A 354 g, 400 g, and 443 g of SH pellets were measured and dissolved in 646 g, 600 g, and 557 g of clean water based on the chemistry procedures established by Rajamane and Jeyalakshmi [46] for the preparation of 12 M, 14 M, and 16 M activators, respectively. The SH solutions were prepared 24 h earlier to reduce the high rise in temperature owing to the reaction between SH pellets and water and added to SS gel 2 h before casting for better performance, using a SS/SH ratio of 2.5: 1.

The locally sourced aggregates were used and prepared at saturated surface conditions before the mix design. Grading was also conducted on the aggregates to obtain the needed particle size distribution (PSD). Moreover, the aggregates were characterized in line with the BS EN 12,620 [47]. The specific gravity (SG), water absorption (WA) and moisture content (MC) of the aggregates were determined following the procedure stated in BS EN 12,620 [47]. The results showed the SG of 2.60 g/cm^3 and 2.64 g/cm^3; WA of 0.7 % and 0.8 %, and MC of 0.3 % and 0.2 % for both fine aggregate (FA) and coarse aggregate (CA), respectively. Fig. 3 shows the PSD of both FA and CA used; the aggregates satisfied the limits of BS EN 12,620 [47]. On the other hand, the mineralogical composition of the coarse aggregate (granite) was identified with the aid of the Petrological Microscope, Model RPI-3 T. The sample was prepared, polished in a glass ground plate using a carborundum, and mounted on a clean glass slide with adhesive [48]. Also, the chemical composition was analyzed using the XRF spectrometer machine, Philips PW-1800. The results of mineralogical composition showed quartz, feldspar, mica, and iron oxide of 62.50 %, 20.45 %, 16.55 %, and 0.50 %, respectively. Moreover, the chemical composition reveals SiO_2, Al_2O_3, Fe_2O_3, CaO, MgO, SO_3, K_2O, Na_2O, P_2O_5, MnO, and LOI as 67.05 %, 14.40 %, 5.63 %, 3.90 %, 1.72 %, 0.02 %, 5.50 %, 1.16 %, 0.15 %, 0.05 %, and 0.52 %, respectively. From these results, it is inferred that the coarse aggregate is acidic granite because the content of SiO_2 was in the range of 66–75% [35]. Besides, based on alkalinity, the granite was classified as calcalkalinity in that $(Na_2O + K_2O)^2/(SiO_2 - 43)$ was 1.85; this

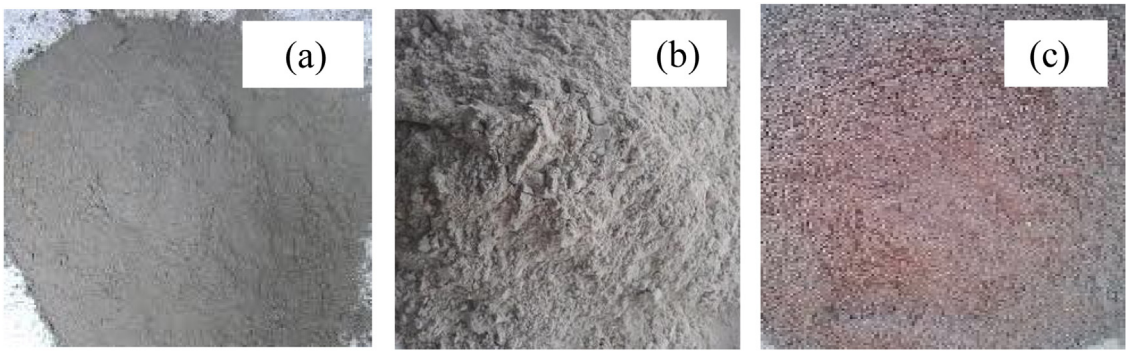

Fig. 1. Binding materials used (a) PLC (b) GGBFS (c) CCA.

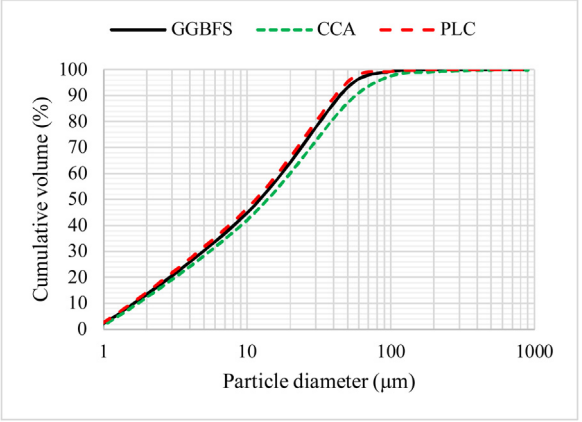

Fig. 2. The cumulative particle size distribution of binding materials used.
LL is the lower limit, UL is an upper limit, FA is fine aggregate, and CA is coarse aggregate

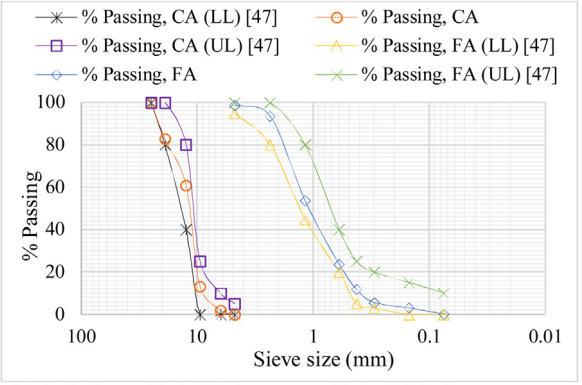

LL is the lower limit, UL is an upper limit, FA is fine aggregate, and CA is coarse aggregate

Fig. 3. The particle size distribution of aggregates used.

ranged between 1.2–3.5 for calcalkalinity [35]. XRF analysis was not performed on the FA because it comprises SiO_2 content, almost in its entirety [48].

2.2. Tests for pozzolanic activity

2.2.1. Strength activity index (SAI)

The SAI was determined in line with the BS 3892−1 [40]. The water to binder ratio was modified to allow for the same flow properties with reference-cement mortar cubes [49], hence requiring mixing water of 235 mL of distilled water. Therefore, the SAI was determined for both 7 days and 28 days compressive strengths (CS) on the average of three samples using the relationship, as illustrated in Eq. 1 [40].

$$\text{SAI, \%} = \frac{P}{C} \times 100 \tag{1}$$

where P is the average CS of pozzolan-reference cement mortar cubes (in MPa)

C is the average CS of reference-cement mortar cubes (in MPa).

The cement-reference mortar cubes, at 7 days and 28 days, showed the CS of 40.64 MPa and 50.43 MPa, respectively. Following the formula, as illustrated in Eq. 1, the test pozzolan (CCA) exhibited a SAI of 0.85 and 0.91 at 7 days and 28 days, respectively, thus showing considerable pozzolanic activity because SAI is greater than 0.80, as recommended by BS 3892−1 [40].

2.2.2. Frattini test (FT)

The FT was analyzed following the procedure specified by BS EN 195−5 [50]. The theoretical maximum concentration (TMC) of [CaO] was determined using the relationship, as illustrated in Eq. 2 [50]. As shown in Table 1, the [CaO] was compared with TMC [CaO], and the result was determined as the difference between the two values, expressing as a percentage of TMC removed. The pozzolanic activity of CCA, as shown in Table 1, removed the lime with 51 %, thus indicating that CCA is pozzolanically active.

$$\text{TMC}\,[\text{CaO}] = \frac{350}{[\text{OH}] - 15} \tag{2}$$

2.3. Tests for hydraulic activity

2.3.1. Slag activity index

The method was carried out following the procedure in ASTM C 989 [39] for the GGBFS. The procedure is similar to that of SAI stated in BS 3892−1 [40] except for 50 % cement replacement, C_3A content ranging from 6 to 10 %, and a maximum of 3% SO_3 content specified by the standards for the reference cement. Therefore, from the XRF results, PLC exhibits 2.03 % SO_3 content, hence satisfying the maximum requirement of 3%. Besides, C_3A was quantified based on Bogue's equation, as shown in Eq. 3 [34]. Based on the XRF result and in line with Eq. 3, the result exhibited 10 % C_3A, thus fulfilling the maximum specification of 10 %. Finally, the slag activity index was determined following the relationship, as illustrated in Eq. 1.

$$C_3A = 2.65(Al_2O_3) - 1.69(Fe_2O_3)\ (\tag{3}$$

The CS of GGBFS-reference cement mortar cubes to the cement-reference mortar cubes with the mean particle size ($d_v50 = 20.68\ \mu m$) exhibited the slag activity index of 76.42 % and 98.53 % at 7 days and 28 days, respectively, hence classifying as grade 100 because the activity index is more than 70 % and 90 % at 7 days and 28 days, respectively [39].

2.3.2. Caustic soda test (CST)

This method was carried out following the procedure outlined in ASTM C 1073−18 [42]. The diluted solution-to-GGBFS ratio was fixed at 0.5 and used to prepare 40 mm × 40 mm × 160 mm prismatic samples. After 6 h and 24 h, all samples were demoulded and tested for CS. The results, average of three test samples, indicated 7.63 MPa and 14.52 MPa at 6 h and 8 h, respectively, hence satisfying the specifications of 7 MPa to 8 MPa and 12 MPa to 15 MPa after 6 h and 8 h, respectively, as recommended by ASTM C 1073−18 [42].

2.4. Materials characterization

The oxide compositions of binding materials, CCA, GGBFS, and PLC, were analyzed using the XRF spectrophotometer machine, Philips PW-1800. The results are shown in Fig. 4. The results revealed that CCA satisfied the chemical pozzolanic requirements stipulated by BS EN 450−1 [51] and BS EN 8615−2 [52] such that the addition of SiO_2, Al_2O_3, and Fe_2O_3 met 70 % minimum requirement. The content of CaO within the range of 10–20% established by Al-Akhras [53] was also met. It can be deduced that the CCA could exhibit a pozzolanic reaction and used as the SCM in the production of blended GPC. On the other hand, GGBFS met the BS EN 15167−1 [38]'s limit requirements of 32–40% for both silica (SiO_2) and lime (CaO) contents. Besides, $(CaO + MgO/SiO_2) \geq 1$, $(CaO/SiO_2) \leq 1.4$, and $SiO_2 + CaO + MgO \geq 67$ % stipulated by BS EN 15167−1 [38] were also met. Also, the oxide compositions obtained herein for GGBFS showed similar compositions with the previous studies [19,31]. Therefore, an inference is made that GGBFS utilized in this study could exhibit both pozzolanic and self-cementitious reactivity, hence suitable for use. In the same vein, the PLC fulfilled the chemical requirements specified by BS EN 196−2 [54].

The microstructural behaviour of the binding materials, GGBFS, CCA, and PLC, was examined using the SEM machine, JEOL 7000600, to establish the characteristics that influenced the RIs of each binder. The SEM analysis was performed on a flat (general) scan. For the investigation, the accelerated voltage was constant at 15 kV, while images were observed at 4000x magnification in a high vacuum. The SEM micrograph results are presented in Fig. 5(a), to a limited extent, reveals a wrinkled internal structure with sharp needles. However, Fig. 5(b) shows an amorphous structure, while Fig. 5 (c) reveals a crystalline and spherical structure.

Table 1
Results of FT at 8 days.

Sample	[OH] mmol l^{-1}	[CaO] mmol l^{-1}	TMC [CaO] mmol l^{-1}	[CaO] reduction (%)
Control	56.83	8.25	8.37	0.70
CCA	39.72	4.63	14.16	50.72

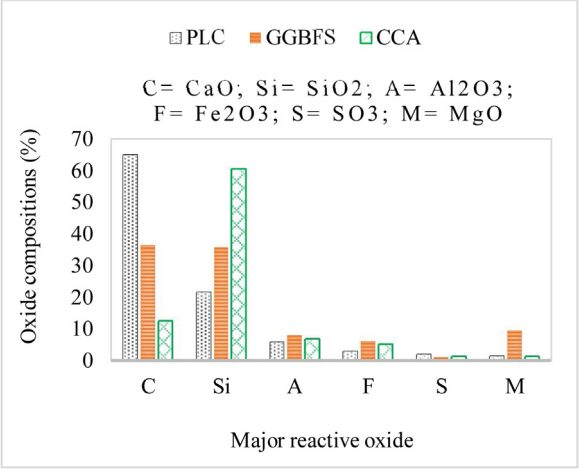

Fig. 4. Chemical compositions of binding materials used.

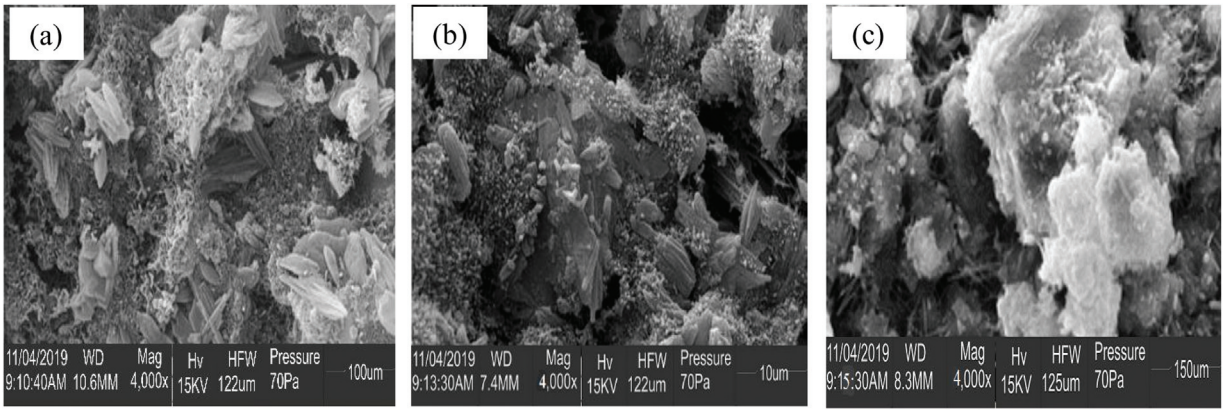

Fig. 5. SEM micrographs on binding materials (a) PLC (b) GGBFS (c) CCA.
E0 (100 % PLC), E1 (100 % GGBFS), E2 (80 % GGBFS + 20 % CCA), E3 (60 % GGBFS + 40 % CCA), E4 (40 % GGBFS + 60 % CCA), E5 (20 % GGBFS + 80 % CCA), and E6 (100 % CCA),

2.5. Mix design quantities

The mix quantities were designed following the procedures stated by BS EN 206 [55]. The percentage replacement of GGBFS by CCA was selected to examine the replacement levels, which would meet the target strengths for both structural and non-load bearing applications. Owing to this, GGBFS was replaced with CCA at 0%, 20 %, 40 %, 60 %, 80 %, and 100 % for the production of GPC and was respectively indicated as E1, E2, E3, E4, E5, and E6, while the PCC (100 % PLC) was indicated as E0. The mix was designed to attain target strengths 30 MPa and 40 MPa for grades M 30 and M 40 concrete, respectively. The mix design quantities for both M 30 and M 40 are shown in Tables 2 and 3, respectively.

2.6. Mix preparation, casting and curing

The dry constituents were prepared following the procedures prescribed by BS 1881–125 [56] and BS EN 12390–2 [57] by preparing and pouring fresh concrete into a cubical mould of 150 mm^3 for compressive strength test, and 150 mm × 600 mm long beam for flexural strength test. The fresh sample was randomly compacted each in three layers, cured under 25 °C and 65 % RH. The compressive strength was tested at 90 days curing, while the flexural strength was tested at 7, 28, 56, and 90 days.

Table 2
Mix quantities for M 30 (in Kg/m^3).

Mix ID	PLC	GGBFS	CCA	FA	CA	SH	SS	SS/SH
E0	390	0	0	675	1031	0	0	0
E1	0	390	0	675	1031	60	150	2.5
E2	0	312	78	675	1031	60	150	2.5
E3	0	234	156	675	1031	60	150	2.5
E4	0	156	234	675	1031	60	150	2.5
E5	0	78	312	675	1031	60	150	2.5
E6	0	0	390	675	1031	60	150	2.5

w/b is the water to binder ratio = 0.54; b/agg is the binder to aggregate ratio = 0.23.

Table 3
Mix quantities for M 40 (in Kg/m^3).

Mix ID	PLC	GGBFS	CCA	FA	CA	SH	SS	SS/SH
E0	500	0	0	585	1031	0	0	0
E1	0	500	0	585	1031	60	150	2.5
E2	0	400	100	585	1031	60	150	2.5
E3	0	300	200	585	1031	60	150	2.5
E4	0	200	300	585	1031	60	150	2.5
E5	0	100	400	585	1031	60	150	2.5
E6	0	0	500	585	1031	60	150	2.5

w/b is the water to binder ratio = 0.42; b/agg is the binder to aggregate ratio = 0.31.

2.7. Experimental tests and analysis

2.7.1. Mechanical test

The compressive strength (f_c) and flexural strength (f_r) were determined with the aid of an INSTRON 5000R UTM following the procedures stated by BS EN 12390−4 [58] and BS EN 12390−5 [59] in a constant force regime under a loading rate of 0.6 MPa and 0.06 MPa per second, respectively. Three (3) samples were made and crushed for each mix ID, and the average was used for the analysis.

2.7.2. Reactivity indexes (RIs) of binding materials

The RIs of binding materials were evaluated using the principal reactive oxides such as CaO, SiO_2, Al_2O_3, Fe_2O_3, MgO, and SO_3 following the establishment of their oxide compositions, which reflect both self-cementitious and pozzolanic reactivity [14,18,32]. The concept which guides the RIs is illustrated in Eq. 4–8 as reactivity, hydraulic, lime, silica, and alumina moduli of each and blended binder, indicating as RM, HM, LM, SM, and AM, respectively.

$$RM = \frac{CaO + MgO + Al_2O_3}{SiO_2} \tag{4}$$

$$HM = \frac{CaO}{SiO_2 + Al_2O_3 + Fe_2O_3} \tag{5}$$

$$LM = \frac{1.0CaO - 0.7SO_3}{2.8SiO_2 + 1.1Al_2O_3 + 0.7Fe_2O_3} \tag{6}$$

$$SM = \frac{SiO_2}{Al_2O_3 + Fe_2O_3} \tag{7}$$

$$AM = \frac{Al_2O_3}{Fe_2O_3} \tag{8}$$

2.7.3. Prediction of f_r based on RIs and MDPs

For this study, MDPs are indicated as water to binder (w/b) ratio and binder to aggregate (b/agg) ratio. Either reactivity, hydraulic, or lime moduli quantifies the self-cementitious properties of each and blended binding material while the pozzolanic activity is quantified by both silica and alumina moduli [32,37]. Consequently, a linear relationship exists in the prediction of f_r and RIs. Thus, the regression was first modelled based on the combination of RM, SM, and AM; HM, SM, and AM; and LM, SM, and AM using Minitab 17 statistical software. Furthermore, in determining the f_r of blended concrete, the RIs of blended binders were integrated and normalized with an inverse of w/b ratio; hence, f_r becomes a direct proportion to RIs, but an inverse proportion to w/b ratio [14,18]. Therefore, the fit regression relationship between fc and w/b ratio was first normalized and modelled in the range of 0.54 to 0.42 w/b ratio for grades M 30 to M 40 concrete, respectively. The f_r and RIs were selected as the response (dependent variable) and continuous predictors (independent variables), respectively, to predict the design data in Minitab 17.

The binder to aggregate (b/agg) ratio also contributed a vital role to the evaluation and improvement of the concrete strength apart from RIs and w/b ratio [14]. The f_r of blended binders was significantly improved when RIs, w/b ratio, and b/agg were all used for the strength correlation. It is noteworthy to state that the volume ratio was used to model the b/agg ratio against the weight ratio. For each mix, the volume fraction was determined using its moisture content and specific gravity to improve the binder-aggregate packing capacity. Following the incorporation of w/b ratio, the fit regression relationship between f_r and b/agg ratio was modelled in the range of 0.31 to 0.23 b/agg ratio for grades M 30 to M 40 concrete, respectively. Consequently, f_r was predicted based on the RIs and MDPs, as illustrated in Eq. 9–11.

$$f_r = \beta + \left(\frac{\alpha_1 RM + \alpha_2 SM + \alpha_3 AM}{w/_b}\right)\left(b/_{agg}\right) \tag{9}$$

$$f_r = \beta + \left(\frac{\alpha_1 HM + \alpha_2 SM + \alpha_3 AM}{w/_b}\right)\left(b/_{agg}\right) \tag{10}$$

$$f_r = \beta + \left(\frac{\alpha_1 LM + \alpha_2 SM + \alpha_3 AM}{w/_b}\right)\left(b/_{agg}\right) \tag{11}$$

where β, α_1, α_2, α_3 represent the magnitudes of coefficients.

2.7.4. Durability test

The chemical resistance was conducted on the prepared cube samples using the solutions of sulphuric acid (H_2SO_4) at 2% concentration [34,60] for acidic attacks. The concrete specimens were tested for both weight and strength loss after 90 days of immersion in H_2SO_4.

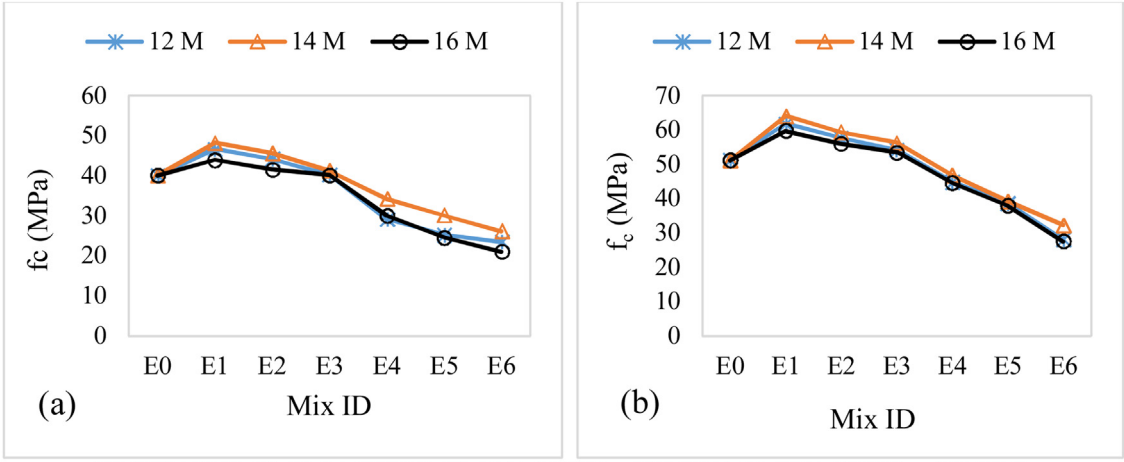

E0 (100% PLC), E1 (100% GGBFS), E2 (80% GGBFS + 20% CCA), E3 (60% GGBFS + 40% CCA), E4 (40% GGBFS + 60% CCA), E5 (20% GGBFS + 80% CCA), and E6 (100% CCA),

Fig. 6. Compressive strength (a) M 30 (b) M 40.

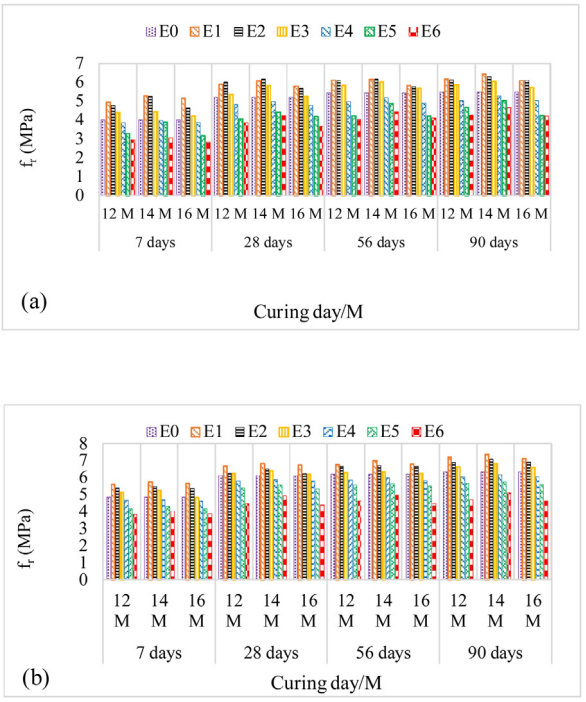

Fig. 7. Flexural strengths (a) M 30 (b) M 40.

3. Results and discussion

3.1. Mechanical properties

Figs. 6 and 7 present the results of both compressive and flexural strengths, respectively. From Figs. 6 and 7, the results revealed both compressive and flexural strengths increased with increasing GGBFS content for both M 30 and M 40 at all curing days, respectively. The results could be associated with the reaction between the aluminosilicate glassy phases (amorphous structure) of GGBFS, as shown in Fig. 5(b), and the alkaline solutions, hence resulting in x-ray amorphous aluminosilicate paste (X-RAAP). The X-RAAP, according to Criado et al. [61], contributes to the higher strengths of the hardened product, compared with both wrinkled and crystalline structures for PCC and CCA, as shown in Fig. 5(a) and (c), respectively. Besides, unlike 12 M and 16 M activators, 14 M activator exhibited the highest compressive and flexural strengths at all curing days because of its capacity to liberate more aluminosilicate gels in the mix. However, at 16 M activating level, the OH^- solution in the mix could be excessive, thus encasing the amorphous paste, causing a barrier to the activating dissolution, and delaying the hydrating agent (calcium-silicate-aluminate-hydrate, C-S-A-H) in the mixed paste; this delays and decreases the strengths.

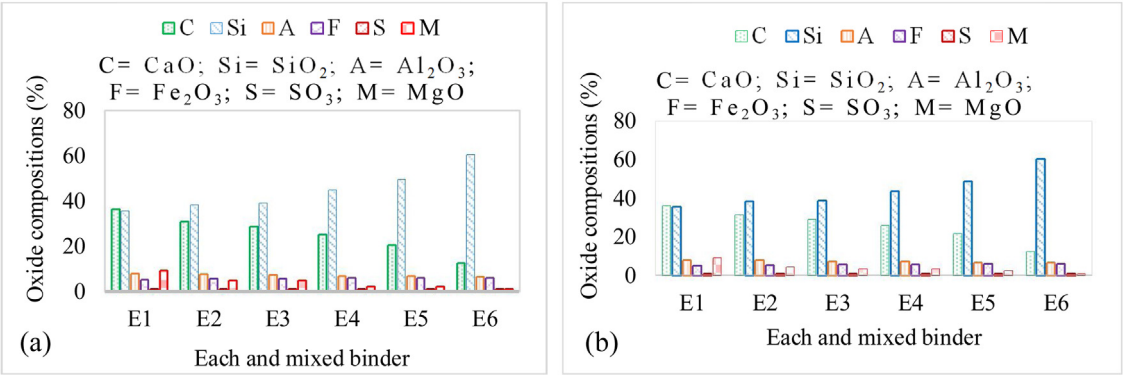

Fig. 8. Principal reactive oxides of each and mixed binder for (a) M 30 and (b) M 40.

3.2. Principal reactive oxides of blended binders

Fig. 8 shows a decrease in CaO, Al_2O_3, and MgO with increasing CCA content, while SiO_2, Fe_2O_3, and SO_3 increase with increasing CCA content in the blended mix; this supports the similar findings reported by Akinwumi and Aidomoje [17] that the reactive oxides, CaO, MgO, and Al_2O_3 decrease with increasing CCA content, while SiO_2, Fe_2O_3, and SO_3 increase with increasing CCA content for the CCA-PC blend. Meanwhile, Behim et al. [32] and Demoulian et al. [36] stated that GGBFS exhibits a similar mineralogical composition to PC; it majorly possesses oxides of Ca, Si, Al, Mg, and Fe, and this gives GGBFS its hydraulic and pozzolanic properties. Also, Xia and Visintin [14] and Darquennes [33] opined that slag is said to exhibit both self-cementitious and pozzolanic properties if the content of CaO and SiO_2 is higher than 30 %. From the XRF results of GGBFS, it is clear that the contents of both CaO and SiO_2 are higher than 30 %. On the other hand, Taylor [62] and Hewlett [63] reported that the self-cementitious reaction of slag decreases as the crystalline content in the blended mix increases; this demonstrates that the reactivity of GGBFS depends on the increasing content of its amorphous structure, and the significant oxides which contribute to the high phase of an amorphous structure are oxides of Ca, Al, and Mg [64,65]. Thus, through close examination of microstructures of binding materials, as shown in Fig. 5, it was evident that the content of the amorphous structure in GGBFS could gradually decrease while the content of the crystalline structure in CCA might increase when GGBFS is replaced with CCA. Consequently, as the content of CCA in the blended mix increases, CaO, Al_2O_3, and MgO in GGBFS decrease. In contrast, SiO_2, Fe_2O_3, and SO_3 in CCA increase; this corroborates the findings from relevant studies in that the reactivity of GGBFS increases with increasing CaO, MgO, and Al_2O_3 contents but reduces as the contents of SiO_2, Fe_2O_3, and SO_3 rise [66,67]. However, it was pointed out that GGBFS comprises small crystal material and is advantageous to its reactivity [68–70]. Besides, Gruskovanjak et al. [67] pointed out that the optimum content of the principal reactive oxides of slag is more beneficial to its self-cementitious reactivity than the content of the amorphous structure. Therefore, it is inferred that the contents of CaO, Al_2O_3, MgO, SiO_2, Fe_2O_3, and SO_3 influence the reactive potentials of GGBFS–CCA blended binders.

3.3. RIs of the blended mix

In assessing the RIs of each blended binder, Eq. 4–5 was used, and the results are shown in Fig. 9. It was revealed that the RM, HM, LM, and AM decreased with increasing CCA content, while the SM increased with increasing CCA content in the blended mix for both M 30 and M 40. Besides, it was evident from the results that CaO, Al_2O_3, MgO, SiO_2, Fe_2O_3, and SO_3 influenced the RIs of the blended binders. The RM, HM, and LM of the blended binders increased with increasing CaO, Al_2O_3, MgO contents, while the SM and AM of the blended binders increased as the contents of SiO_2 and Al_2O_3 increased, respectively. In contrast to HM, the RM of the blended binders met the minimum requirement of 1.0 specified by BS EN 8615–2 [52]. Statistically, the RM, HM, LM, and AM of the blended mix decreased from 25 to 78 %, 19–77%, 19–77%, and 11–26% as the percentage replacement of CCA by GGBFS increased from 20 % to 100 % for both M 30 and M 40, respectively. The self-cementitious properties of mixed binders increase with an increase in CaO, Al_2O_3, and MgO contents, thus resulting in stronger hydraulic reactions [32,71]. As a result, the decrease in RIs may be attributed to the reduction in principal reactive oxides, CaO, Al_2O_3, and MgO as a result of the increase in CCA content in the blended mix. However, the SM of the blended mix decreased from 44 to 10 % as the percentage replacement of CCA by GGBFS rose from 20 to 100 % for both M 30 and M 40, respectively. Meanwhile, it is shown in Fig. 7 that CCA, being a pozzolan, exhibits higher content of silica (SiO_2) compared with that of GGBFS. Therefore, this result confirms the findings reported by Mathhes et al. [70] that SM increases with increasing SiO_2 content, hence resulting in stronger pozzolanic properties. On the other hand, the reactivity of

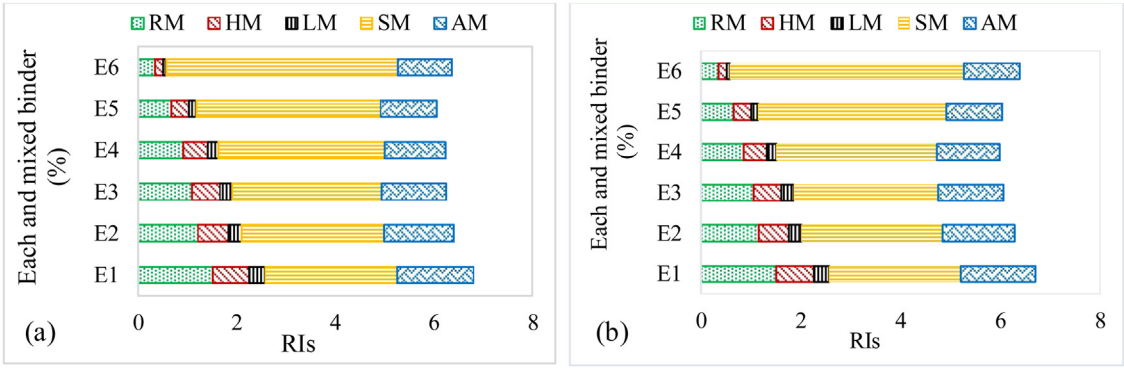

Fig. 9. RIs of each and mixed binder for (a) M 30 and (b) M 40.

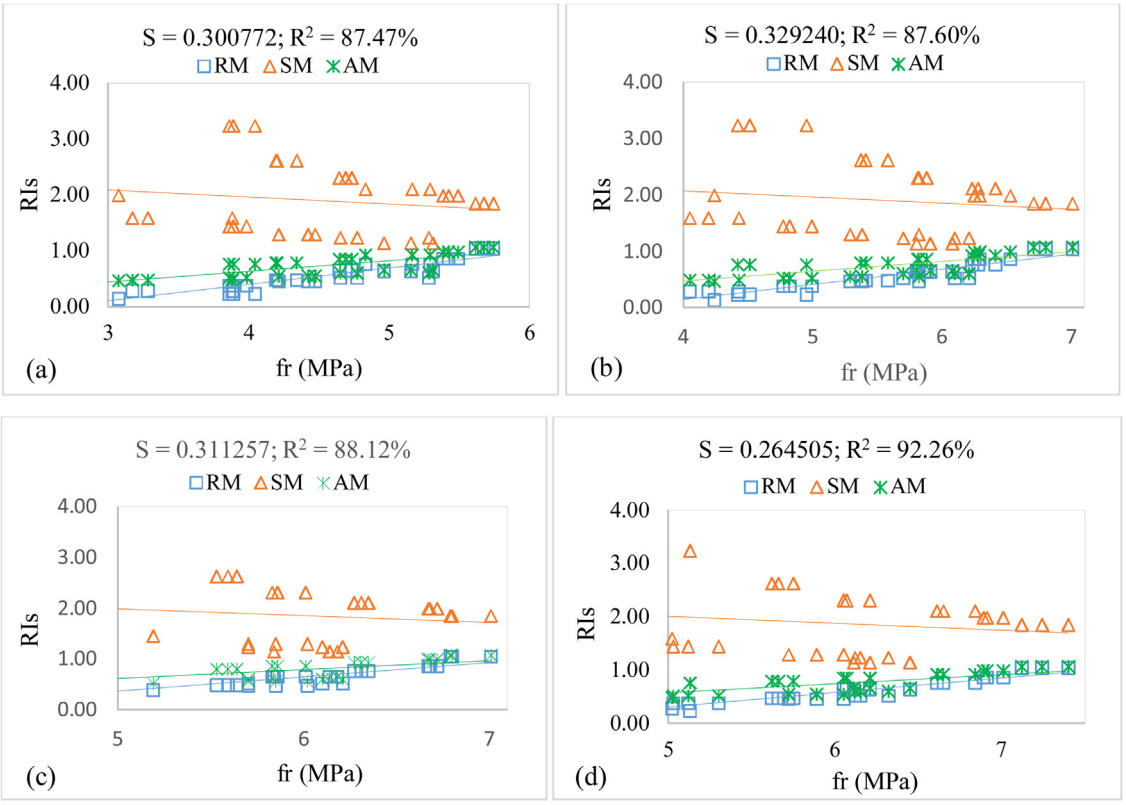

Fig. 10. Statistical data for RM, AM, SM, and MDPs (a) 7 (b) 28 (c) 56 and (d) 90 days.

GGBFS depends on its amorphous structure, thus influencing its RIs [69,70]. This assertion confirms the SEM micrographs, as shown in Fig. 5 (b) and (c) for GGBFS and CCA, which display amorphous and crystalline structures, respectively.

3.4. Prediction of f_r based on RIs and MDPs

3.4.1. Prediction of f_r based on RM, AM, SM, and MDPs

Following Eq. 9, the results of the statistical data are shown in Fig. 10 (a)-(d) for 7, 28, 56, and 90 days, respectively. It was observed that some data points for SM significantly deviated from the regression line. This may be asserted to the diversity of chemical compositions of blended binders, aggregate type and volume, and mix design proportions; this assertion confirms the findings reported by Xie and Visintin [21] and Neville [34] that differences in the oxide composition of blended binders, aggregate types, texture, and shape, and methods of mix design, affect the data results, hence influencing the reactive potentials of blended concrete incorporating SCMs. Moreover, the flexural strength increased with increasing RM and AM but decreasing SM; this may be attributed to the higher contents of CaO and Al_2O_3 in GGBFS, which increases RM and AM, thus resulting in a stronger self-cementitious reaction. However, the higher content of SiO_2 in CCA increases its SM, hence leading to a pozzolanic reaction rather than a hydraulic reaction; this also confirms the findings of a similar study reported by Gruskovnjak et al. [67] that the RM and AM increase as the CaO and Al_2O_3 contents increase, while SiO_2 content reduces, thus resulting in high reactivity. However, the higher contents of SiO_2 and low contents of CaO and Al_2O_3 result in low reactivity. On the other hand, a blended mix with high contents of CaO, Al_2O_3, and MgO exhibits high self-cementitious/hydraulic properties in the presence of alkaline activators [66,68,70].

The fit regression model was used for the correlation of f_r based on the RIs (RM, AM, and SM) and MDPs at the global trend of 95 % confidence interval (CI) and prediction interval (PI). Thus, the regression equations are illustrated in Eq. 12–15 for 7, 28, 56, and 90 days, respectively. Therefore, the coefficient of determination (R^2) is 87.47 %, 87.60 %, 88.12 %, and 92.26 % fit to predict the data at 95 % CI and PI for 7, 28, 56, and 90 days, respectively, thus

indicating 0–5.20% increase in R^2 as the curing age increases from 7–90 days. Ultimately, relative to RIs and MDPs, these developed models can be used for the strength prediction of concrete incorporating SCMs.

$$f_{r-7\ days} = \left\{\frac{7.81\,AM - 1.468\,SM - 2.63\,RM}{\frac{w}{b}}\right\}\left(\frac{b}{agg}\right) + 3.028 \tag{12}$$

$$f_{r-28\ days} = \left\{\frac{2.22\,AM - 0.440\,SM + 1.66\,RM}{\frac{w}{b}}\right\}\left(\frac{b}{agg}\right) + 3.825 \tag{13}$$

$$f_{r-56\ days} = \left\{\frac{2.82\,AM - 0.5975\,SM + 1.10\,RM}{\frac{w}{b}}\right\}\left(\frac{b}{agg}\right) + 4.125 \tag{14}$$

$$f_{r-90\ days} = \left\{\frac{4.91AM - 0.969\,SM - 0.13\,RM}{\frac{w}{b}}\right\}\left(\frac{b}{agg}\right) + 4.193 \tag{15}$$

3.4.2. Prediction of f_r based on HM, AM, SM, and MDPs

Fig. 11 (a)-(d) indicates the statistical data for HM, AM, SM, and MDPs at 7, 28, 56, and 90 days, respectively. It was observed that some data points of SM were out of the regression line due to the difference in binders' oxide compositions, the volume and chemical compositions of aggregates, and mix proportions. Besides, the f_r of GGBFS–CCA blended concrete increased with increasing HM and AM but decreasing SM. The reason for a higher strength cannot be far-fetched: GGBFS exhibits higher content of CaO and Al_2O_3 compared with CCA, hence resulting in stronger hydraulic reaction, but this hydraulic reaction decreases when replaced with CCA, which predominantly contains a higher content of SiO_2. This assertion is in line with the findings reported in various studies that the hydraulic response of slag reduces with increasing silica content [64,65]. Therefore, it is inferred that the HM of GGBFS–CCA blended binder increases with higher contents of CaO and Al_2O_3 and the lower content of SiO_2 in the mix.

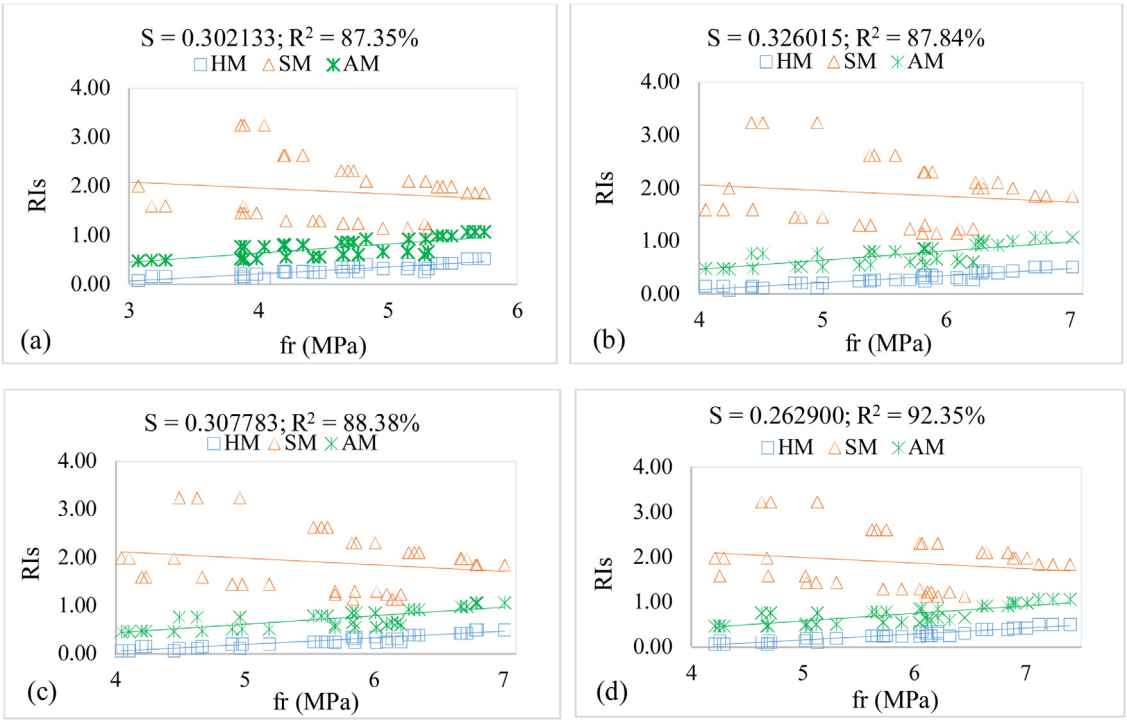

Fig. 11. Statistical data for HM, AM, SM, and MDPs (a) 7 (b) 28 (c) 56 and (d) 90 days.

The fit regression model was used for the correlation of f_r based on the RIs (HM, AM, and SM) and MDPs at the 95 % CI and PI, and the regression equations are illustrated in Eq. 16–19 for 7, 28, 56, and 90 days, respectively. Thus, at 7, 28, 56 and 90 days, R^2 is 87.35 %, 87.84 %, 88.38 %, and 92.35 % fit to correlate the data, respectively. Statistically, there is 0–5.4% increase in R^2 as the curing age increases from 7 to 90 days.

$$f_{r-7\ days} = \left\{\frac{5.50\,AM - 1.036\,SM - 1.99\,HM}{\frac{w}{b}}\right\}\left(\frac{b}{agg}\right) + 3.022 \tag{16}$$

$$f_{r-28\ days} = \left\{\frac{2.60\,AM - 0.521\,SM + 2.82\,HM}{\frac{w}{b}}\right\}\left(\frac{b}{agg}\right) + 3.814 \tag{17}$$

$$f_{r-56\ days} = \left\{\frac{2.59\,AM - 0.565\,SM + 2.59\,HM}{\frac{w}{b}}\right\}\left(\frac{b}{agg}\right) + 4.111 \tag{18}$$

$$f_{r-90\ days} = \left\{\frac{3.69\,AM - 0.753\,SM + 1.49\,HM}{\frac{w}{b}}\right\}\left(\frac{b}{agg}\right) + 4.178 \tag{19}$$

3.4.3. Prediction of f_r based on LM, AM, SM, and MDPs

The statistical data for LM, AM, SM, and MDPs are indicated in Fig. 12 (a)-(d) for 7, 28, 56, and 90 days, respectively. It was noticed that some data points of SM were out of the global trend due to the diversity in oxide compositions, aggregates volumes and types, and mix proportions of the blended binders. Moreover, the f_r of GGBFS–CCA blended concrete increased with increasing LM and AM but decreasing SM; this may be attributed to the fact that GGBFS exhibits higher content of CaO and Al_2O_3 compared with CCA, hence resulting in a stronger reactive component. Still, this reactive component decreases

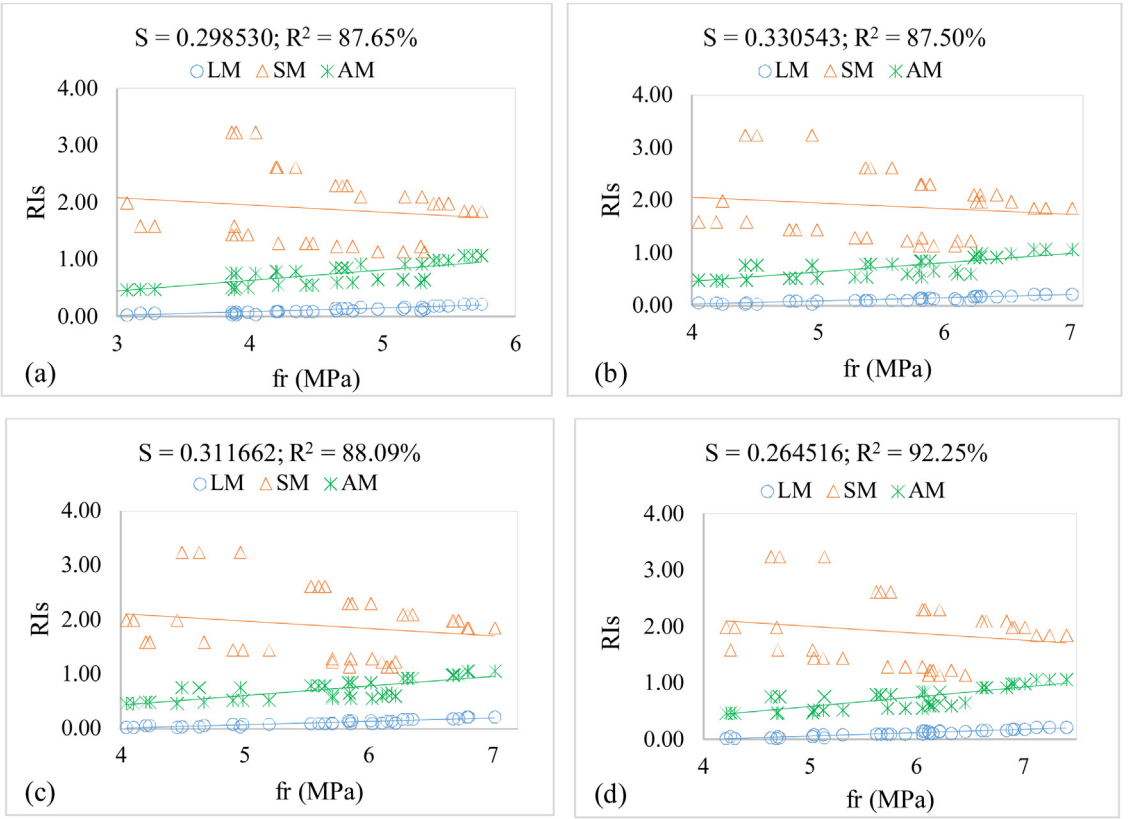

Fig. 12. Statistical data for LM, AM, SM, and MDPs (a) 7 (b) 28 (c) 56 and (d) 90 days.

when replaced with CCA, which majorly contains a higher content of silica. Therefore, it is inferred that the LM of GGBFS−CCA blended binder increases with higher contents of CaO and Al_2O_3 and the lower content of SiO_2 in the mix.

The f_r, RIs (LM, AM, and SM), and MDPs were predicted using the fit regression model at the 95 % CI and PI, and the regression equations are illustrated in Eq. 20–23 for 7, 28, 56, and 90 days, respectively. Therefore, at 7, 28, 56, and 90 days, R^2 is 87.50 %, 87.65 %, 88.09 %, and 92.25 % fit to correlate data, respectively, hence indicating 0–5.20% increase in R^2 as the curing age increases from 7 to 90 days. Finally, with respect to RIs and MDPs, these proposed models can be used for the strength prediction of concrete incorporating SCMs.

$$f_{r-7\ days} = \left\{\frac{6.51\,AM - 1.250\,SM - 7.74\,LM}{\frac{w}{b}}\right\}\left(\frac{b}{agg}\right) + 3.044 \tag{20}$$

$$f_{r-28\ days} = \left\{\frac{4.21\,AM - 0.802\,SM + 1.07\,LM}{\frac{w}{b}}\right\}\left(\frac{b}{agg}\right) + 3.835 \tag{21}$$

$$f_{r-56\ days} = \left\{\frac{3.87\,AM - 0.786\,SM + 1.62\,LM}{\frac{w}{b}}\right\}\left(\frac{b}{agg}\right) + 4.127 \tag{22}$$

$$f_{r-90\ days} = \left\{\frac{4.74\,AM - 0.938\,SM - 0.04\,LM}{\frac{w}{b}}\right\}\left(\frac{b}{agg}\right) + 4.192 \tag{23}$$

3.4.4. Comparison of experimental results with predicted values

Fig. 13 illustrates the statistical comparison and trend between the flexural strengths of experimental results and that of predictive values. It was observed that both empirical and predictive results exhibited similar values and patterns of flexural strength. In contrast to HM, both LM and RM showed the best fit at all levels of curing time for both M 30 and M 40. These observations confirm the findings reported in similar studies such that LM yields the best fit for PC blended with cashew nut shell ash (CNSA) [18]. In contrast, RM yields the best fit for blended concrete incorporating SCMs [14]. Despite producing the

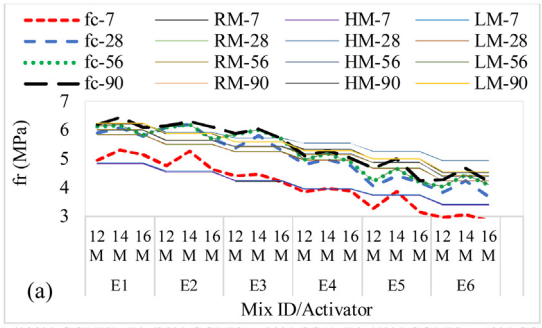

E1 (100% GGBFS), E2 (80% GGBFS + 20% CCA), E3 (60% GGBFS + 40% CCA), E4 (40% GGBFS + 60% CCA), E5 (20% GGBFS + 80% CCA), and E6 (100% CCA),

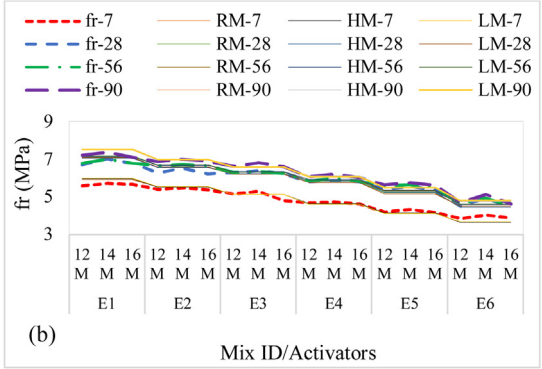

Fig. 13. Comparison of experimental results with predicted values (a) M 30 (b) M 40.

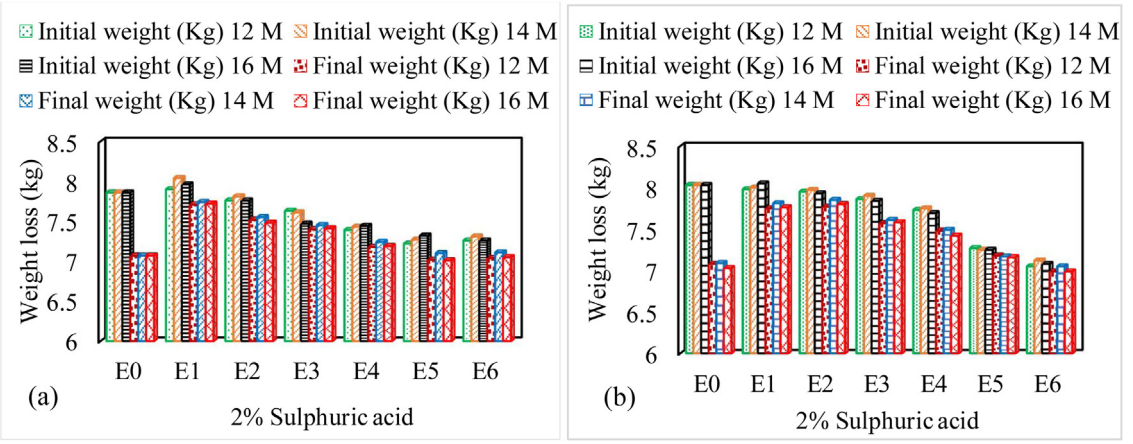

Fig. 14. Weight loss of cubes immersed in 2% H_2SO_4 for 90 days (a) M 30 (b) M 40.
E0 (100 % PLC), E2 (100 % GGBFS), E2 (80 % GGBFS + 20 % CCA), E3 (60 % GGBFS + 40 % CCA), E4 (40 % GGBFS + 60 % CCA), E5 (20 % GGBFS + 80 % CCA), and E6 (100 % CCA),

similar values and trends of flexural strength at all levels of curing time, it was evident from Fig. 9 that LM of the GGBFS–CCA blended binders was low compared with the minimum requirements ($\geq 0.66 \leq 1.02$) recommended by BS EN 197–1 [72]; besides, HM was less than 1 compared with the minimum requirement (< 1) specified by BS EN 197–1 [72]. However, RM satisfied the minimum requirement (< 1) defined by Behim et al. [32], Demoulian et al. [36], and BS EN 15167–1 [38]. The variations in LM and HM may be attributed to the difference in chemical and mix properties of concrete in that BS EN 197–1 [72]'s recommendation was based on the PC blended binders such that the ratio of CaO to SiO_2 in the blended mix was high compared with GGBFS–CCA blended binders reported in this study. Therefore, it is inferred that RM yields the best fit for GGBFS–CCA blended binder, and this can be used in the validation of blended binders incorporating SCMs.

3.5. Chemical attacks

Owing to the immersion of selected samples on 2% H_2SO_4 solution for 90 days, Fig. 14 (a) and (b) present the weight loss for both M 30 and M 40, respectively, while Fig. 15 (a) and (b) present the compressive strength (f_c) loss for both M 30 and M 40, respectively. It was observed that the percentage weight loss in GPC samples, for both M 30 and M 40, ranged from 1 to 2% against 10–13% in PCC samples, while the percentage strength loss in GPC, for both M 30 and M 40, varying from 1 to 5% as against 12–14% in PCC samples after 90 days exposure of concrete samples in 2% H_2SO_4. These results confirm the similar findings reported by Sanni and Khadiranaikar [25], Malhotra et al. [73], and Singh et al. [74] that the percentage weight loss and strength loss in GPC samples was less than 5% against 15 % in PCC samples after 90 days of exposure in 2% H_2SO_4. The

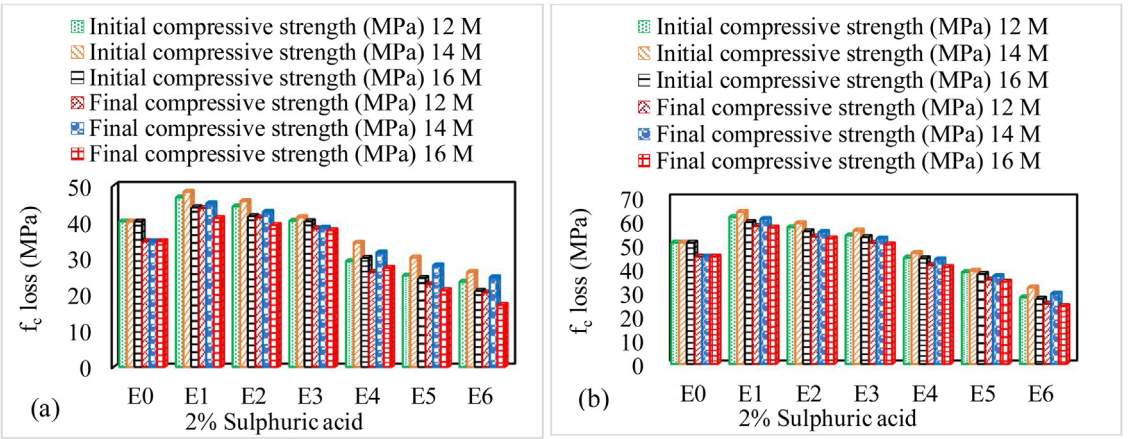

E0 (100% PLC), E2 (100% GGBFS), E2 (80% GGBFS + 20% CCA), E3 (60% GGBFS + 40% CCA), E4 (40% GGBFS + 60% CCA), E5 (20% GGBFS + 80% CCA), and E6 (100% CCA),

Fig. 15. Strength loss of cubes immersed in 2% H_2SO_4 for 90 days (a) M 30 (b) M 40.

deterioration may be attributed to the aggressive attack of H_2SO_4 on $Ca(OH)_2$ and C-S-H of PCC structure. In contrast, the C-S-A-H on GPC structure is protected and fixed by the presence of diluted water-glass (sodium silicate), thus forming calcium silicates which filled the pores [23,25,34]. Therefore, it is inferred that GGBFS–CCA blended GPC offers better resistance to acidic attack than PCC.

E1 (100 % GGBFS), E2 (80 % GGBFS + 20 % CCA), E3 (60 % GGBFS + 40 % CCA), E4 (40 % GGBFS + 60 % CCA), E5 (20 % GGBFS + 80 % CCA), and E6 (100 % CCA),

4. Conclusion

The study examined the GGBFS–CCA-based GPC, and its effects on the activity indexes and the acidic attacks were evaluated. Both experimental and statistical methods were used in the course of the study, and the results were compared with PCC. Consequent upon the findings and in line with research aims, the following sets of conclusions are made:

- The reactivity of GGBFS–CCA blended binder increases with increasing CaO, MgO, and Al_2O_3 contents. However, the reactivity decreases with increasing SiO_2, Fe_2O_3, and SO_3 contents.
- The RM, HM, and LM of GGBFS–CCA blended binder increases with increasing CaO, MgO, and Al_2O_3 contents, while the SM and AM increase with increasing SiO_2 and Al_2O_3 contents.
- Flexural strength of GGBFS–CCA GPC increases with increasing RM, HM, LM, and AM
- RM yields the best fit for predicting the flexural strength of slag-based GPC, incorporating CCA compared with HM and LM. Besides, a good correlation exists between the experimental results and proposed model equations.
- There is a remarkable improvement in R^2 as the curing age increases.
- Slag-based GPC incorporating CCA provides excellent acidic resistance superior to that of PCC.

The concept of activity moduli in predicting the f_r of the GGBFS–CCA blended mix is attainable. This study benefits future research by focusing on three prospective solutions. First, the proposed model equations can be useful in the prediction and application of strength design proportions for GPC incorporating agro-industrial by-products under ambient curing conditions provided the chemical compositions are obtained. Second, the efficiency of the fit regression model in predicting f_r based on the RIs and the MDPs is affirmed. Third, the application of agro-industrial by-products, GGBFS and CCA, can be advantageous in a highly acidic environment.

Declaration of Competing Interest

The authors show a credit to the sources in the manuscript. The authors declare that they have no known competing for financial interests or personal relationships that could have appeared to influence the work reported in this paper. The raw/processed data required to reproduce these findings cannot be shared at this time as the Data also forms part of an ongoing study. The authors declare that the manuscript is the authors' original work and has not been published before. The authors also declare that the article contains no libellous or unlawful statements and does not infringe on the rights of others.

Acknowledgements

The researchers thank the Covenant University Centre for Research, Innovation, and Discovery (CUCRID) for the provision of the fund and conducive environment in carrying out the study.

References

[1] E. Aprianti, P. Shafigh, S. Bahri, J.N. Farahani, Supplementary cementitious materials origin from agricultural wastes: a review, Constr. Build. Mater. 74 (2015) 176–187.
[2] E.M. Fairbairn, B.B. Americano, G.C. Cordeiro, T.P. Paula, R.D. Toledo Filho, M.M. Silvoso, Cement replacement by sugar cane bagasse ash: CO_2 emissions reduction and potential for carbon credits, J. Environ. Manag. 91 (9) (2010) 1864–1871.
[3] R. Feiz, J. Ammenberg, L. Baas, M. Eklund, A. Helgstrand, R. Marshall, Improving the CO_2 performance of cement, part I: utilizing life-cycle assessment and key performance indicators to assess development within the cement industry, J. Clean. Prod. 98 (2015) 272–281.
[4] L.K. Turner, F.G. Collins, Carbon dioxide equivalent (CO_2-e) emissions: a comparison between geopolymer and OPC cement concrete, Constr. Build. Mater. 43 (2013) 125–130.
[5] S. Mahmoudkelaye, K.T. Azari, M. Pourvaziri, E. Asadian, Sustainable material selection for building enclosure through ANP method, Case Stud. Const. Mater. 9 (2018)e00200.
[6] X. Bai, R.J. Dawson, D. Ürge-Vorsatz, G.C. Delgado, A.S. Barau, S. Dhakal, Six research priorities for cities and climate change, Nature 555 (7694) (2018) 23–25.
[7] A.R.G. de Azevedo, J. Alexandre, E.B. Zanelato, M.T. Marvila, Influence of incorporation of glass waste on the rheological properties of adhesive mortar, Constr. Build. Mater. 148 (2017) 359–368.
[8] H. Jahanbakhsh, M.M. Karimi, H. Naseri, N.F. Moghadas, Sustainable asphalt concrete containing high reclaimed asphalt pavements and recycling agents: performance assessment, cost analysis, and environmental impact, J. Clean. Prod. 244 (2020)118837.
[9] S. Ghavami, H. Jahanbakhsh, A. Saeedi Azizkandi, N.F. Moghadas, Influence of sodium chloride on cement kiln dust-treated clayey soil: strength properties, cost analysis, and environmental impact, Environ. Dev. Sustain. 22 (2020) 1–20.
[10] S. Dadsetan, J. Bai, Mechanical and microstructural properties of self-compacting concrete blended with metakaolin, ground granulated blast furnace slag and fly ash, Constr. Build. Mater. 146 (2017) 658–667.
[11] T. Xie, T. Ozbakkaloglu, Influence of coal ash properties on compressive behaviour of FA-and BA- based GPC, Mag. Concr. Res. 67 (24) (2015) 1301–1314.

[12] P.S. Deb, P. Nath, P.K. Sarker, in: S. Yazdani, A. Singh (Eds.), Properties of Fly Ash and Slag Blended Geopolymer Concrete Cured at Ambient Temperature, New Dev. Struct. Eng. Constr., ISEC-7, Honolulu, 2013, pp. 18–23 June.
[13] K. Mohamed, R. Mateus, L. Bragança, Comparative sustainability assessment of binary blended concretes using supplementary cementitious materials (SCMs) and ordinary Portland cement (OPC), J. Clean. Prod. 220 (2019) 445–459.
[14] T. Xie, P. Visintin, A unified approach for mix design of concrete containing supplementary cementitious materials based on reactivity moduli, J. Clean. Prod. 203 (2018) 68–82.
[15] A.A. Raheem, S.O. Oyebisi, S.O. Akintayo, M.O. Oyeniran, Effects of admixture on the properties of corncob ash cement concrete, Leonardo Electron, J. Pract. Technol. 16 (2010) 13–20.
[16] S. Oyebisi, A. Ede, O. Ofuyatan, J. Oluwafemi, I. Akinwumi, Comparative study of corncob ash-based lateritic interlocking and sandcrete hollow blocks, Int. J. Geomate 15 (51) (2018) 209–216, doi:http://dx.doi.org/10.21660/2018.51.45918.
[17] I.I. Akinwumi, O.I. Aidomojie, Effect of corncob ash on the geotechnical properties of lateritic soil stabilized with Portland cement, Int. J. Geomat. Geosci. 5 (3) (2015) 375–392.
[18] S. Oyebisi, T. Igba, D. Oniyide, Performance evaluation of cashew nutshell ash as a binder in concrete production, Case Stud. Constr. Mater. 11 (2019) e00293.
[19] S.E. Aprianti, A huge number of artificial waste material can be supplementary cementitious material (SCM) for concrete production - a review part II, J. Clean. Prod. 142 (2017) 4178–4194.
[20] O. Ofuyatan, A. Ede, R. Olofinnade, S. Oyebisi, T. Alayande, J. Ogundipe, Assessment of strength properties of cassava peel ash-concrete, Int. J. Civ. Eng. Technol. 9 (1) (2018) 965–974.
[21] S. Oyebisi, A. Ede, F. Olutoge, T. Igba, J. Ramonu, Rheology of slag-based geopolymer concrete using corncob ash as a pozzolanic material, IOP Conf. Series: Mater. Sci. Eng. 640 (2019)012057, doi:http://dx.doi.org/10.1088/1757-899X/640/1/012057.
[22] P. Nath, P.K. Sarker, Effect of GGBFS on setting, workability and early strength properties of fly ash geopolymer concrete cured in ambient condition, Constr. Build. Mater. 66 (2014) 163–171.
[23] A. Ramezanianpour, H.B. Jovein, Influence of metakaolin as supplementary cementing material on strength and durability of concretes, Constr. Build. Mater. 30 (2012) 470–479.
[24] G. Hannesson, K. Kuder, R. Shogren, D. Lehman, The influence of high volume of fly ash and slag on the compressive strength of self-consolidating concrete, Constr. Build. Mater. 30 (2012) 161–168.
[25] S.H. Sanni, R. Khadiranaikar, Performance of geopolymer concrete under severe environmental conditions, Int. J. Civ. Struct. Eng. 3 (2) (2012) 396–407.
[26] S. Oyebisi, A. Ede, F. Olutoge, O. Ofuyatan, T. Alayande, Building a sustainable world: economy index of geopolymer concrete, 10th Int, Struct. Eng. Constr. Conf. (ISEC-10) (2019) ISBN: 978-0-9960437-6-2.
[27] J. Thaarrini, S. Dhivya, Comparative study on the production cost of geopolymer and conventional concretes, Int. J. Civ. Eng. Res. 7 (2) (2016) 117–124.
[28] United States Department of Agriculture, World Agricultural Production, Circular Series Wap 08-17, Office of Global Analysis, International Production Assessment Division, South Building, Washington DC, 2018.
[29] A. Hammoudi, K. Moussaceb, C. Belebchouche, F. Dahmoune, Comparison of artificial neural network (ANN) and response surface methodology (RSM) prediction in compressive strength of recycled concrete aggregates, Constr. Build. Mater. 209 (2019) 425–436.
[30] A.K. Al-Shamiri, J.H. Kim, T.F. Yuan, Y.S. Yoon, Modeling the compressive strength of high-strength concrete: an extreme learning approach, Constr. Build. Mater. 208 (2019) 204–219.
[31] J. Sobhani, M. Najimi, A.R. Pourkhorshidi, T. Parhizkar, Prediction of the compressive strength of no-slump concrete: a comparative study of regression, neural network and ANFIS models, Constr. Build. Mater. 24 (2010) 709–718.
[32] M. Behim, M. Beddar, P. Clastres, Reactivity of granulated blast furnace slag, Slovak J. Civ. Eng. 21 (2) (2013) 7–14.
[33] A. Darquennes, B. Espion, S. Staquet, Assessing the hydration of slag cement concretes, Constr. Build. Mater. 40 (2013) 1012–1020.
[34] A.M. Neville, Properties of Concrete, fifth ed., Pearson Education Ltd., England, 2011.
[35] A. Rittman, Using the Rittman serial index to define the alkalinity of igneous rocks, E Schwetzerbartsche Vealagsbuchandlung Stuttgart 184 (1) (1962) 95–103.
[36] E. Demoulian, P. Gourdin, F. Hawthorn, C. Vernet, Influence of slags chemical composition and texture on their hydraulicity, Paris, FR, Proceedings from Seventh International Conference on the Chemistry of Cement, 21980, pp. 89.
[37] S. Donatello, M. Tyrer, C.R. Cheeseman, Comparison of test methods to assess pozzolanic activity, Cem. Concr. Compos. 32 (2010) 121–127.
[38] British Standard E.N. 15167-1, Ground Granulated Blast Furnace Slag for use in Concrete, Mortar and Grout: Definitions, Specifications, and Conformity Criteria, BSI, London, 2006.
[39] American Society for Testing and Materials C 989, Standard Specification for Ground Granulated Blast-furnace Slag for use in Concrete and Mortars, Annual Book of ASTM Standards, Philadelphia, PA, 2004.
[40] British Standard 3892-1, Pulverized-Fuel Ash: Specification for Pulverized Fuel Ash for use with Portland Cement, BSI, London, 1997.
[41] British Standard E.N. 196-5, Methods of Testing Cement: Pozzolanicity Test for Pozzolanic Cement, BSI, London, 2011.
[42] American Society for Testing and Materials C1073-18, Standard Test Method for Hydraulic Activity of Slag Cement by Reaction with Alkali, ASTM International, West Conshohocken, PA, 2018.
[43] American Society for Testing and Materials C-618, Standard Specification for Coal Fly Ash and Raw or Calcined Natural Pozzolan for use in Concrete, Annual Book of ASTM Standards, Philadelphia, PA, 2005.
[44] British Standard E.N. 196-3, Method of Testing Cement: Physical Test, BSI, London, 2016.
[45] British Standard E.N. 196-6, Methods of Testing Cement: Determination of Fineness, BSI, London, 2018.
[46] N.P. Rajamane, R. Jeyalakshmi, Quantities of Sodium Hydroxide Solids and Water to Prepare Sodium Hydroxide Solution of Given Molarity for Geopolymer Concrete Mixes, Indian Concrete Institute Technical Paper, SRM University, India, 2014.
[47] British Standard E.N. 12620, Aggregates from Natural Sources for Concrete, BSI, London, 2013.
[48] G.I. Obiefuna, P.H. Sini, A. Maunde, Geochemical and mineralogical composition of granitic rock deposits of Michika area North East, Nigeria, Int. J. Sci. Technol. Res. 7 (4) (2018) 160–170.
[49] British Standard E.N. 1015-3, Methods of Test for Mortar for Masonry: Determination of Consistence of Fresh Mortar (by Flow Table), BSI, London, 1999.
[50] British Standard E.N. 196-5, Methods of Testing Cement: Pozzolanicity Test for Pozzolanic Cement, BSI, London, 2005.
[51] British Standard E.N. 450-451, Pozzolan for use in Concrete: Definitions, Specifications, and Conformity Criteria, BSI, London, 2012.
[52] British Standard E.N. 8615-2, Specification for Pozzolanic Materials for use with Portland Cement: High Reactivity Natural Calcined Pozzolana, BSI, London, 2019.
[53] N.M. Al Akhras, Durability of metakaolin concrete to sulfate attack, Cem. Concr. Res. 36 (9) (2006) 1727–1734.
[54] British Standard E.N. 196-2, Methods of Testing Cement: Chemical Analysis of Cement, BSI, London, 2016.
[55] British Standard EN 206, Concrete Specifications, Performance, Production and Conformity, BSI, London, 2016.
[56] British Standard 1881-125, Testing Concrete: Methods for Mixing and Sampling Fresh Concrete in the Laboratory, BSI, London, 2013.
[57] British Standard E.N. 12390-12392, Testing Hardened Concrete: Making and Curing for Strength Tests, BSI, London, 2019.
[58] British Standard E.N. 12390-12394, Testing Hardened Concrete: Compressive Strength of Test Specimens, BSI, London, 2019.
[59] British Standard EN 12390 -5, Testing Hardened Concrete: Flexural Strength of Test Specimens, BSI, London, 2019.
[60] British Standard E.N. 16523-1, Determination of Material Resistance to Permeation by Chemicals, Under the Conditions of Continuous Contact, BSI, London, 2015.
[61] M. Criado, A. Fernandez-Jimenez, A.G. de la Torre, M.A.G. Aranda, A. Palomo, An XRD study of the effect of the SiO2/Na2O ratio on the alkali activation of fly ash, Cem. Concr. Res. 37 (2008) 671–679.

[62] H.F. Taylor, Cement Chemistry, Thomas Telford, London, 1997.
[63] P. Hewlett, Lea's Chemistry of Cement and Concrete, third ed., John Wiley & Sons Inc., New York, 2003, pp. 635–663.
[64] R.D. Hooton, Canadian use of ground granulated blast-furnace slag as supplementary cementing material for enhanced performance of concrete, Canadian J. Civ. Eng. 27 (4) (2000) 754–760.
[65] R.D. Hooton, J.J. Emery, Glass content determination and strength prediction for vitrified blast furnace slag, ACI SP-79 (2) (1983) 943–962.
[66] J.C. Yang, Chemistry of slag-rich cements, Tokyo, Proceedings of the Fifth International Symposium on the Chemistry of Cement, 41969, pp. 296–309.
[67] A. Gruskovnjak, B. Lothenbach, F. Winnefeld, B. Münch, R. Figi, S.C. Ko, U. Mäder, Quantification of hydration phases in super sulfated cement: review and new approaches, Adv. Cem. Res. 23 (6) (2011) 265–275.
[68] S. Pal, A. Mukherjee, S. Pathak, Investigation of hydraulic activity of ground granulated blast furnace slag in concrete, Cem. Concr. Res. 33 (9) (2003) 1481–1486.
[69] H.G. Smolczyk, Slag structure and identification of slags, Proceedings from the 7th ICCC, 1: Cong. Chem. Cem. 1, Paris, 1980, pp. 1–3.
[70] W. Matthes, A. Vollpracht, Y. Villagrán, S. Kamali-Bernard, D. Hooton, E. Gruyaert, M. Soutsos, N. De Belie, Ground granulated blast-furnace slag, in: N. De Belie, M. Soutsos, E. Gruyaert (Eds.), Properties of Fresh and Hardened Concrete Containing Supplementary Cementitious Materials State-of-the-Art Report of the RILEM Technical Committee 238-SCM, Working Group 4, first ed., Springer International Publishing, 2018, pp. 2–46.
[71] F. Winnefeld, M. Ben Haha, G. Le Saout, M. Costoya, S.C. Ko, B. Lothenbach, Influence of slag composition on the hydration of alkali-activated slags, J. Sust. Cem. Mater. 4 (2) (2015) 85–100.
[72] British Standard EN 197-1, Cement: Composition, Specifications and Conformity Criteria for Common Cements, British Standard Institution, 2 Park Street, London, 2016.
[73] V.M. Malhotra, M.H. Zhang, P.H. Read, J. Ryell, Long-term mechanical properties and durability characteristics of high-strength/high-performance concrete incorporating supplementary cementing materials under outdoor exposure conditions, Mate. J. 97 (5) (2000) 518–525.
[74] B. Singh, G. Ishwarya, M. Gupta, S.K. Bhattacharyya, Geopolymer concrete: a review of some recent developments, Constr. Build. Mater. 85 (2015) 78–90.